

3D Dental Biometrics: Automatic Pose-invariant Dental Arch Extraction and Matching

Xin ZHONG

Social Cognitive Computing Department

Institute of High Performance Computing

Agency for Science, Technology and Research (A*STAR)

Fusionopolis, 138632, Singapore

andreayoung123@gmail.com

Zhiyuan ZHANG

Digital Manufacturing and Design Centre

Singapore University of Technology and Design

8 Somapah Road, 487372, Singapore

cszyzhang@gmail.com

Abstract—A novel automatic pose-invariant dental arch extraction and matching framework is developed for 3D dental identification using laser-scanned dental plasters. In our previous attempt [1-5], 3D point-based algorithms have been developed and they have shown a few advantages over existing 2D dental identifications. This study is a continuous effort in developing arch-based algorithms to extract and match dental arch feature in an automatic and pose-invariant way. As best as we know, this is the first attempt at automatic dental arch extraction and matching for 3D dental identification. A Radial Ray Algorithm (RRA) is proposed by projecting dental arch shape from 3D to 2D. This algorithm is fully automatic and fast. Preliminary identification result is obtained by matching 11 postmortem (PM) samples against 200 ante-mortem (AM) samples. 72.7% samples achieved top 5% accuracy. 90.9% samples achieved top 10% accuracy and all 11 samples (100%) achieved top 15.5% accuracy out of the 200-rank list. In addition, the time for identifying a single subject from 200 subjects has been significantly reduced from 45 minutes to 5 minutes by matching the extracted 2D dental arch. Although the extracted 2D arch feature is not as accurate and discriminative as the full 3D arch, it may serve as an important filter feature to improve the identification speed in future investigations.

Index Terms—3D dental biometrics, dental arch, feature extraction, human identification, Radial Ray Algorithm (RRA)

I. INTRODUCTION

Dental biometrics is an irreplaceable branch of biometrics. It can assist in victim identification when other evidence is not available. The reliability of dental records outperforms that of DNA and fingerprint in mass disasters with extreme conditions, e.g. forest fires, tsunami, earthquakes when heat, chemicals and strong forces can easily alter the structure of these identifiers [6-7]. Extensive effort has been put into the research toward dental biometrics in the last two decades and many prominent approaches have been proposed in 2D identification schemes by comparing dental radiographs [8-23]. We have demonstrated in our previous work [1-5] that using 3D features and identification schemes overcomes a number of key problems that plague 2D identification schemes, including 1) blur radiographs make feature extraction difficult; 2) imaging angle change problems make those features inaccurate thus impossible to match against AM records in the database. 3D point-based algorithms have been developed [1-5] and they have shown a few advantages over

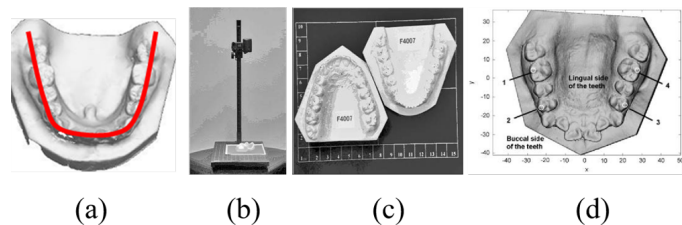


Fig. 1. (a) Dental arch and (b-d) dental arch manual extraction in orthodontic applications [24].

existing 2D dental identifications. This study is a continuous effort in developing arch-based algorithms to extract and match a new dental feature - the dental arch in an automatic and pose-invariant way. This work mainly makes contributions and improvement in the following two aspects: 1. We propose automatic pose-invariant dental arch extraction algorithm and matching framework. As best as we know, ours is the first attempt at automatic dental arch extraction and matching from 3D dental surface models; It saves time for the dentists and it erases the tediousness in traditional manual dental arch extraction. 2. Our method is fully automatic and fast thus it makes rapid identification possible in mass disasters. We have reported that it takes 45 minutes on average to identify one subject from 200 subjects using pointed-based method [1, 3]. In contrast, the arch-based method only takes 5 minutes on average to identify one subject from the same 200 subjects.

II. DENTAL ARCH

The dental arch form has been receiving increasing attention both in dental science [24-26] and engineering [27] for orthodontic applications. By definition, dental arch is the curve formed by the cutting edges and masticating surfaces of the teeth as indicated in Fig. 1 (a). To correct malocclusions and assisting in shaping teeth and jaws, the dental arch provides important reference for dental brace (arch wire) design and customized production in orthodontic applications. Geometric morphology analyses of the dental arch form using

mathematical functions have been reported in literature under a normal occlusion assumption in orthodontic applications, e.g. thin-plate spline, beta function, natural cubic splines, polynomial equations, and Hermite cubic splines. However, manual calibration and specification of feature points on every plaster model are required as illustrated in Fig. 1 (b-d), making mass extraction and fast retrieval of the dental arch infeasible. Although the arch shape is considered to be unique among individuals, the shape of dental arch is distorted in 2D radiographs, thus making it not suitable in 2D identification schemes.

III. SYSTEM APPROACH OVERVIEW AND DATA PREPARATION

An overview of the 3D dental arch identification framework is shown in Fig. 2. Basically, there are three major components in this framework: preprocessing, arch extraction and arch matching.

We created our own 3D dental database at National Security Office. It's confidential at this moment for 3D dental biometrics development in Singapore but we may apply to publish a set of dental records for public testing of the developed algorithm in future. The AM database comprises 200 mandibular samples. The PM samples consist of 11 mandibular samples which are separately prepared and scanned by a different investigator without knowing the previous scanning parameters in order to simulate the differences in real forensic dental identification. As reported in [1], AM samples and PM samples may have different mesh topologies, different orientations and different appearances. All samples are scanned using Minolta VIVID 900 Surface Laser Scanner (Konica-Minolta Corporation, Osaka, Japan). And all PM and AM samples have been decimated and auto-segmented. The decimation and segmentation in the preprocessing step have been presented in details in previous work [1].

IV. DENTAL ARCH EXTRACTION AND MATCHING

The two main components of arch-based matching and identification framework are arch extraction and correspondence. Table I shows the main steps of the Radial Ray Algorithm (RRA) for arch extraction and matching.

As dental samples could have any initial orientation, its orientation should be properly aligned. In previous work [1], the alignment is realized by matching pose invariant feature points. In this study, Principal Component Analysis (PCA) is used to achieve fast alignment before arch extraction. The following steps are implemented for dental arch extraction.

A. PCA Alignment

Align principal axis x, y, z to the respective Euclidian coordinate X, Y, Z. as shown in Fig. 3. Principal axes do not have positive or negative directional property. the dental arch opening direction is either positive Y or negative Y.

TABLE I
MAIN STEPS OF RADIAL RAY ALGORITHM (RRA) FOR ARCH EXTRACTION AND MATCHING

Input: 11 PM surface model and 200 AM surface model Output: 11 rank lists Steps: Arch Extraction - Radial Ray Algorithm (RRA) <ul style="list-style-type: none"> • PCA Alignment of principal axes x, y, z to the Euclidian coordinate X, Y, Z for both PM and AM samples (Fig. 3) • Boundary points computation for both AM and PM samples (Fig. 3) • Arch opening direction constraint I (Fig. 4) • Extract dental arch - middle points of boundary points by RRA (Fig. 5) Arch Feature Description <ul style="list-style-type: none"> • Starting from the middle-extracted points, 10 points on each side are used to describe arch feature. 21 points is specified to describe the more critical anterior arch (Fig. 7) Arch Matching <ul style="list-style-type: none"> • Flip effect constraint: flip extracted PM samples about Y axis (Fig. 8) • Match both original and flipped PM arches to 200 AM arches by calculating rotation and translation using 21 points: Genuine matching (same person) (Fig. 9. top left) and imposter matching (Fig. 9. the other three).

B. Constraint 1: Arch Opening Direction Constraint

To get correct and consistent alignment, the following constraints are applied to get positive Y alignment. 1) Compute the boundary points of the mesh model and project them onto the x-y plane as shown in Fig. 3. 2) The centroid is the origin of the projected boundary points as shown in Fig. 4 (a-b) and the centroid is found to be close to the anterior teeth. **Lmax** denotes the length from the centroid to maximum Y value of boundary points (dash line) and **Lmin** denotes the length from the centroid to minimum Y value of boundary points (solid line) ; 3) If **Lmax < Lmin** (**Lmax** is shorter than **Lmin**) as shown in Fig. 4(a-b), flip boundary points about X axis on X-Y plane. This may create a flipped dental arch about Y axis. This flipped effect will be discussed later. It will be eliminated by adding another constraint (constraint 2 in step E).

C. Extract Dental Arch Points Using the Developed Radial Ray Algorithm

The arch extraction method is developed based on the middle points (black circles in Fig. 5) extraction of boundary points (blue '+' marks in Fig. 5). The following steps are implemented. 1) Specify point B according to centroid A as shown in Fig. 5. L_{AB} is defined as the length between point B and the centroid A. L_{AB} is 70% of the total length L (**Lmax+Lmin** in Fig. 4 (a)) of projected points along Y axis. Point B should have a higher Y value than Y maximum of boundary points to guarantee that one radial ray (black lines emitted from B) only intersect with either left jaw teeth boundary or right jaw teeth boundary. The middle points will

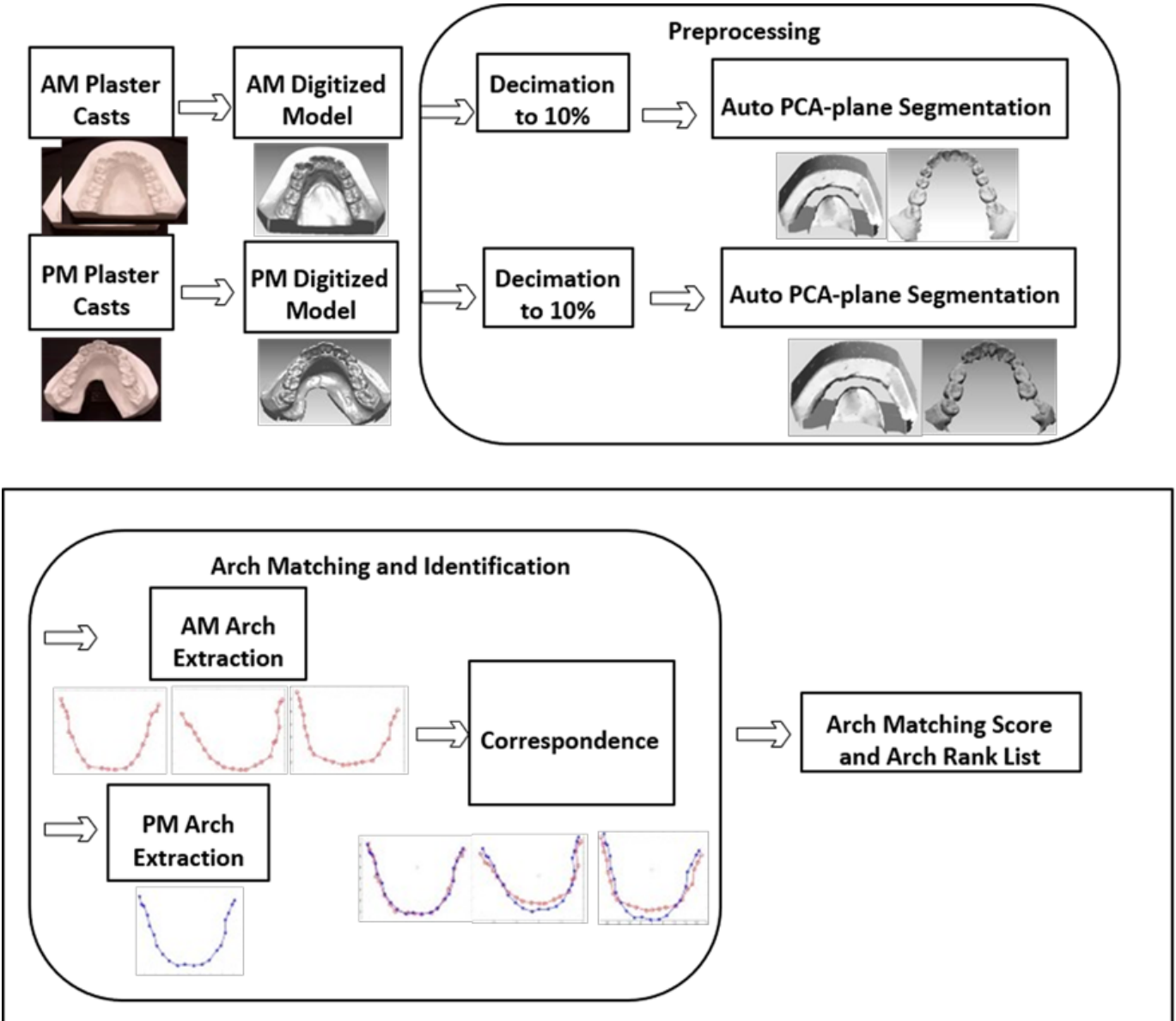


Fig. 2. An overview of 3D dental arch identification framework.

be computed in between the longest intersection ray and the shortest ray in each sub-divided area as shown in Fig. 5. We observed that 70% is the most suitable value for all the samples. 2) then step two: the division into 50 sub-areas is centered at point B. Start from positive X axis, divide the space clockwise into 50 sub-areas from 0 to 180 degree. The number 50 is also determined from observations and experiments. Literature studies [24-26] used 5, 7, 14 points to interpolate a curve to describe the arch shape which showed inadequacy of shape description in Fig. 6 upper row. Fig. 6 upper row shows that if we use the same number of points in literature, the shapes are not smooth enough to describe real arch shapes. It is under-fitting. It is true that more points will give more details of arch shape but it should not be over described either. As the lower row middle and right figures show that when dividing

into 55 and 60 sub-areas, over-fitting effect will appear. In each sub-area, the middle points will be computed as the average of the longest intersection ray and the shortest ray as shown in Fig. 5 and Fig. 6.

D. Arch Feature Description

According to Kieser et al. [28], anterior dentition is in fact unique and critical in describing dental arch shape. As it is shown in Fig. 7, parts of dental cast in the auto-segmented sample is attached at both ends to the sample which does not belong to the dentition. It will be excluded from the dental arch. Starting from the middle-extracted points, 10 points on each side are used during matching. The suitable number of points specified is 21 which is obtained from observations. The 21 specified points include anterior teeth (incisors and

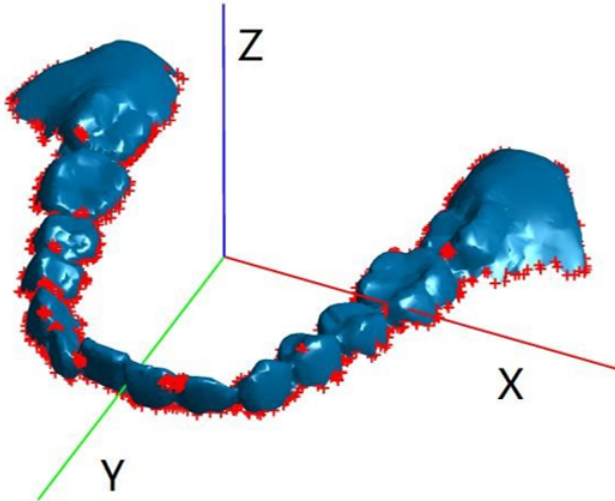


Fig. 3. Aligned 3D surface model with its boundary points (red points).

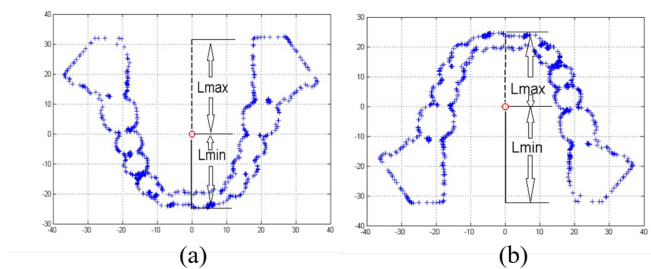


Fig. 4. Arch opening direction constraint.

canines), premolars and the first molar but there is no obvious boundary to separate the last molar with the attached casts. All the arch points below the black line are used in matching. There will be variation from sample to sample, but the 21 points will provide adequate shape description while having the attached dental cast removed.

E. Dental Arch Matching

As Principal axes do not have positive or negative directional property. The extracted arch may also flip about Y axis (left jaw teeth and right jaw teeth flip with each other) after PCA alignment. We mentioned in Step B Constraint 1. Here is Constraint 2 - flip effect constraint. To offset the flip effect, the extracted points are matched first, and then the flipped points are matched again. The points with smaller matching error will be taken as the correct match. The following three steps are implemented to match the dental arch: 1) Calculate AM and PM dental arches and flip the PM dental arch as Fig. 8 shows. AM arch—red line with circle ‘o’ marker; PM arch—blue line with star ‘*’ marker; Flipped PM arch—green line with addition ‘+’ marker. 2) Calculate the rotation matrix using 21 points, align the extracted dental arch then calculate the point-to-point Euclidian distance. The mean distance is the matching error. Fig. 8(a) shows the matching error (0.9109) between AM

TABLE II
ARCH MATCHING RESULT

PM ID	I	II	III	IV	V	VI	VII	VIII	IX	X	XI
Rank	1	2	15	2	2	20	3	1	7	1	31

and PM arches and Fig. 8(b) shows the matching error (0.9459) of AM and flipped PM arches. Those two errors do not have much difference since the jaw teeth has good symmetrical structure (< 1.0 error value as found for genuine matching). Other samples' matching errors may have much larger difference. The smaller error (0.9109) is used to rank dental arch matching results. 3) Repeat the above process until all 200 AM samples have been matched and sort the matching errors in ascending order. The outcome is a ranked list which contains 200 ranks. Fig. 9 shows some examples of the matching error difference when matching genuine samples (PM and AM sample is from the same person) and imposter samples (matching different persons' PM and AM samples). The genuine matching usually has smaller error.

V. EXPERIMENTS RESULTS AND DISCUSSION

A. Results

Table II shows the identification results by matching the 11 PM samples to 200 AM samples. The absolute rank in the 200-rank list is recorded for each PM sample. 72.7% samples achieved top 5% (10/200) accuracy. 90.9% samples achieved top 10% (20/200) accuracy and all 11 samples (100%) achieved top 15.5% (31/200) accuracy out of the 200-rank list.

B. Discussion

PCA Alignment outcomes – As we all know that PCA algorithm doesn't provide directional information. Fig. 10 shows the four possible orientations after PCA alignment.

As Fig. 10 shows, we tried different initial orientations before the PCA alignment (blue models). The grey model are the ones after PCA alignment. We can clearly see that the arch after PCA alignment can flip around x axis (the red axis): Fig. 10 (a) vs Fig. 10(b); Fig. 10(c) vs Fig. 10(d); To solve this, we added Constraint 1: arch opening direction constraint in IV Section B and illustrated in in Fig. 4. Additionally, the arch could also flip around y axis (the green axis), we did not manage to solve this left-right flip directly. We solve this indirectly by adding Constraint 2 (in IV section E) – Y flip effect constraint by matching each PM arch twice (non-flipped PM arch and flipped PM arches in Fig. 8) with the same AM arch. This is the limitation of the developed Radial Ray Algorithm (RRA). However, as the arch extraction and matching is much faster than our previous developed point-based algorithms. It has speed advantages even we need to match twice for each PM arch. We will discuss the identification speed in the following session.

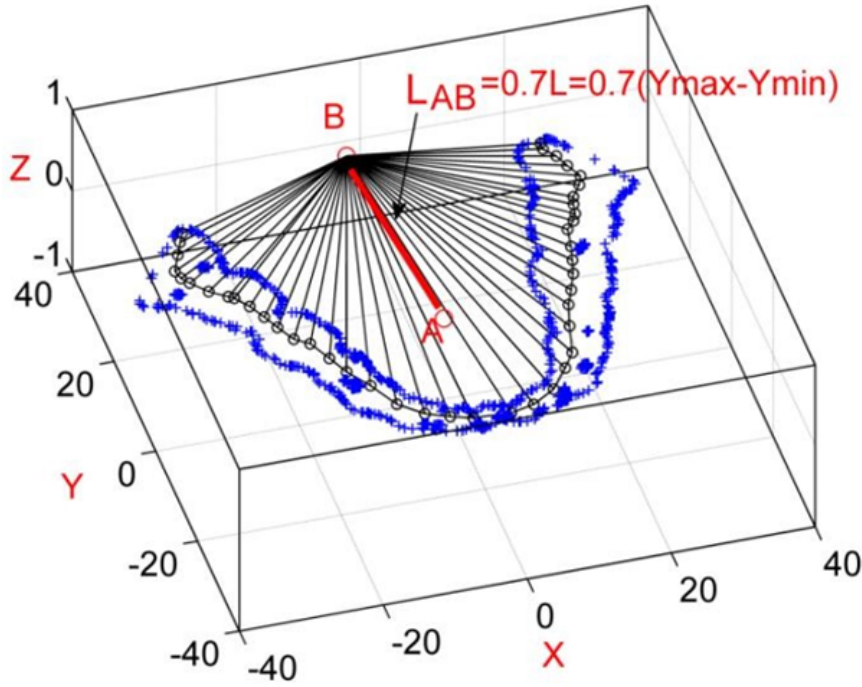


Fig. 5. Radial Ray Algorithm (RRA) and extracted dental arch.

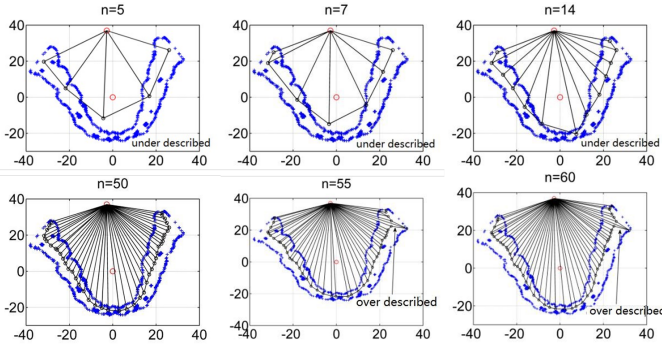


Fig. 6. Under described (upper row) and over described (lower middle and right) dental arches.

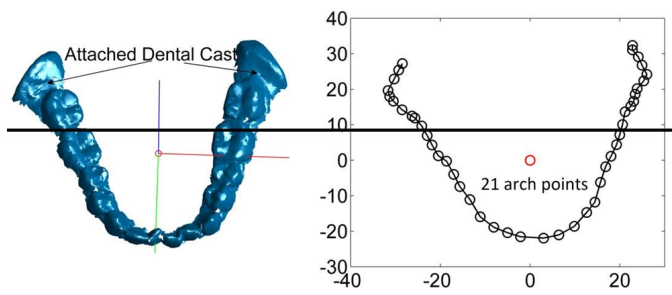


Fig. 7. Extracted anterior arch.

Identification Accuracy - As mentioned, there are inevitable differences during data preparation, such as different initial orientations, different mesh topology and different segmentations.

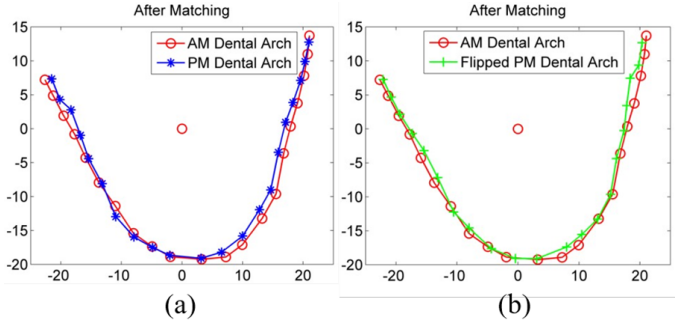


Fig. 8. (a) AM and PM arch matching (b) AM and flipped PM arch matching.

Fig. 11 shows the AM and PM samples belonging to the same person have not been perfectly aligned with each other after PCA alignment which may give a relatively larger matching error ($1.1263 \text{ mm} > 1.0 \text{ mm}$). Maybe that's the reason why we only have 3 PM samples got perfect rank-1 accuracy. We tested that all 11 PM samples achieved Rank -1 accuracy by using our previous developed point-based algorithm [1,3]. Although the extracted 2D arch feature is not as accurate and discriminative as the full 3D arch, it may serve as an important filter feature to improve the identification speed in future investigations.

Identification speed - the time for identifying a single subject from 200 subjects has been significantly reduced from 45 minutes [1] to 5 minutes by matching the extracted 2D dental arch alone. In contrast, it is reported in Chen's thesis that it takes about 7 hours to identify one subject from 133 subjects by matching the X-ray images in 2D [18]. However,

we may also acknowledge that we have better computing hardware and software nowadays which also contributed to the improvement of the identification speed. It is difficult to compare with some literature work as we use different hardware and software tested on different datasets – 2D x-ray identification in literature work versus 3D surface model identification in our work. We didn't find enough recent approaches in literature to compare with, especially in 3D dental biometrics domain and arch extraction from 3D dental models. We can only compare with our previous work on point-based method.

Future work – we have tested the arch-based methods on the complete samples in Fig. 12 (C1-C11), we aim to further improve the proposed method for partial dental model identification as shown in Fig. 11 (P1-P11) in future. It is more challenging to identify the partial samples as we have shown in previous work [2]. It's more difficult to get a good alignment and the accuracy is expected to be lower than that of complete samples. We would like to leave the fusion of the point-based and arch-based methods for future investigations to develop a more robust and efficient 3D dental identification framework. Another interesting question to explore is if the identification scheme can identify there is no such victim in the database. This will require more statistical investigations on the matching errors. Furthermore, we have seen that the dental arch is extremely useful for orthodontic surgery planning. The dental arch line is a critical reference line for the orthodontists to plan the surgery. Additionally, in automatic partial denture design application, dental arch is used to determine the position of the missing/remaining teeth in a jaw. We might extend our applications to relevant domains in future.

ACKNOWLEDGMENT

We thank Faculty of Dentistry, National University of Singapore and National Security Office for providing the dental records. We thank Mr. Christian Schwarz from Universität

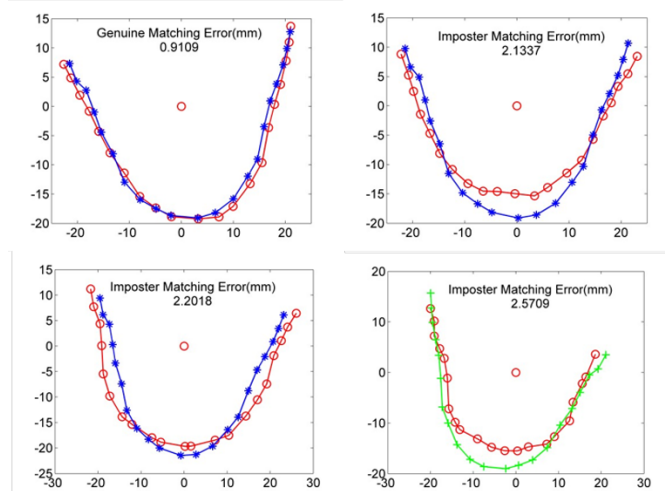


Fig. 9. Difference of genuine arch matching error (top left) and imposter arch matching error (the other three).

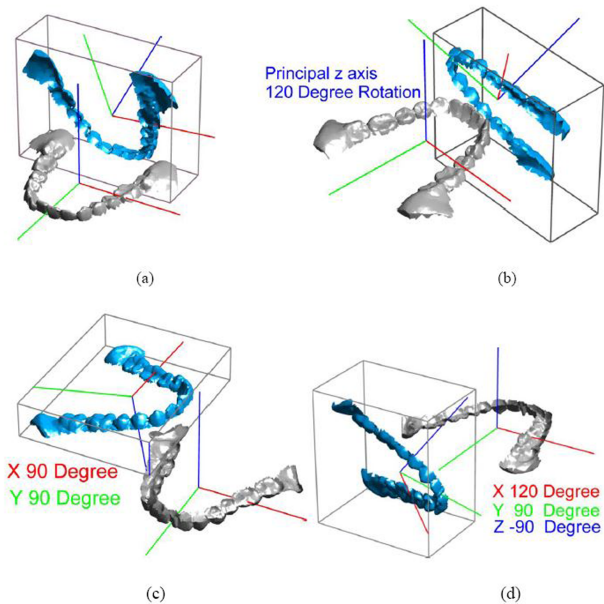


Fig. 10. Four possible orientations after PCA alignment.

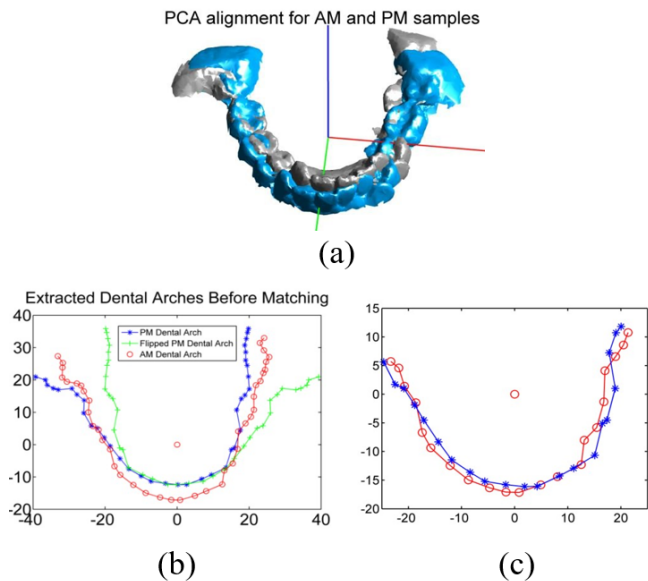


Fig. 11. An example of paired genuine samples are not identified at rank-1 after arch matching (a) PCA alignment of AM and PM samples (b) extracted arches before matching (c) arches after matching.

Karlsruhe (TH) Germany for helping with the establishment of the 3D dental database.

CONFLICT OF INTEREST DISCLOSURE

All authors declare no real or potential conflicts of interest. All authors reviewed the results and drafts, and approved the final manuscript.

REFERENCES

- [1] X. Zhong, D. Yu, K. W. C. Foong, T. Sim, Y. S. Wong, and H. Cheng, "Towards automated pose invariant 3D dental biometrics," pp. 1-7.

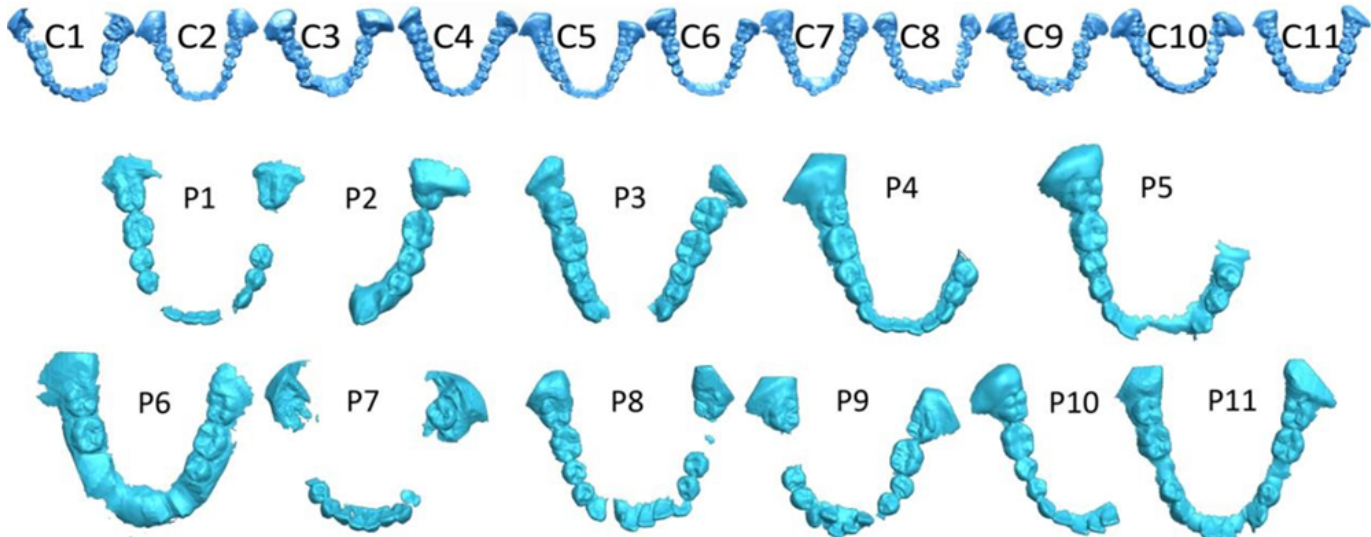


Fig. 12. Complete and partial PM samples.

- International Joint Conference on Biometrics (IJCB), 2011, Washington, D.C.
- [2] X. Zhong, Y. S. Wong, W. F. Lu, K. W. C. Foong, and A. H.-l. Cheng, "A Dental Matching Approach Using Partial Surface Features for Human Identification," Proceedings of the ASME 2012 International Design Engineering Technical Conferences and Computers and Information in Engineering Conference. Volume 2: 32nd Computers and Information in Engineering Conference, Parts A and B. Chicago, Illinois, USA. August 12–15, 2012. pp. 357-366.
 - [3] X. Zhong, D. Yu, Y. S. Wong, T. Sim, W. F. Lu, K. W. C. Foong, and H.-L. Cheng, "3D dental biometrics: Alignment and matching of dental casts for human identification," Computers in Industry, vol. 64, no. 9, pp. 1355-1370, 2013/12/01/, 2013.
 - [4] Z. Zhang, S. H. Ong, X. Zhong, and K. W. C. Foong (2014) An Efficient Partial Shape Matching Algorithm for 3D Tooth Recognition. In: Goh J. (eds) The 15th International Conference on Biomedical Engineering. IFMBE Proceedings, vol 43. Springer, Cham
 - [5] Z. Zhang, S. H. Ong, X. Zhong, and K. W. C. Foong, "Efficient 3D dental identification via signed feature histogram and learning keypoint detection," Pattern Recognition, vol. 60, pp. 189-204, 2016/12/01/, 2016
 - [6] D.R. Senn, P.G. Stimson, Forensic Dentistry, Second Edition ed., CRC Press, Taylor Francis Group, 2010.
 - [7] Dental records beat DNA in tsunami IDs, New Scientists, 2516:12 (2005).
 - [8] G. López, Ó. David, Soft Computing y Visión por Ordenador para la Identificación Forense mediante Comparación de Radiografías, thesis, 2020, <https://digibug.ugr.es/handle/10481/59546>
 - [9] Oktay, Ayse Betul: 'Human identification with dental panoramic radiographic images', IET Biometrics, 2018, 7, (4), p. 349-355, DOI: 10.1049/iet-bmt.2017.0078 IET Digital Library, <https://digital-library.theiet.org/content/journals/10.1049/iet-bmt.2017.0078>.
 - [10] A. E. Rad, M. Shafry, M. Rahim, H. Kolivand, and A. Norouzi, "Automatic computer-aided caries detection from dental x-ray images using intelligent level set," 2018.
 - [11] R. Silva, F. Picoli, S. Carvalho Mendes, P. de Alcantara, T. Botelho, and A. Franco, "Panoramic radiograph as a clue for human identification: A forensic case report," International Journal of Forensic Odontology, vol. 2, no. 2, pp. 85-87, July 1, 2017, 2017.
 - [12] J. Zhou and M. Abdel-Mottaleb, "A content-based system for human identification based on bitewing dental X-ray images," Pattern Recognition., vol. 38, no. 11, pp. 2132–2142, 2005.
 - [13] P. Lin, Y. Lai, and P. Huang, "Dental biometrics : Human identification based on teeth and dental works in bitewing radiographs," Pattern Recognition., vol. 45, no. 3, pp. 934–946, 2012.
 - [14] O. Nomir, S. Member, and S. Member, "HIERARCHICAL DENTAL X-RAY RADIOGRAPHS MATCHING", International Conference on Image Processing, Atlanta, GA, 2006, pp. 2677-2680.
 - [15] O. Nomir, M. Abdel-mottaleb, and S. Member, "Human Identification From Dental X-Ray Images Based on the Shape and Appearance of the Teeth" IEEE Transactions on Information Forensics and Security, vol. 2, no. 2, pp. 188-197, June 2007.
 - [16] O. Nomir and M. Abdel-Mottaleb, "Fusion of Matching Algorithms for Human Identification Using Dental X-Ray Radiographs," in IEEE Transactions on Information Forensics and Security, vol. 3, no. 2, pp. 223-233, June 2008.
 - [17] A. K. Jain, H. Chen, and S. Minut, "Dental Biometrics : Human Identification Using Dental Radiographs" pp. 429–437, Book chapter, Audio- and Video-Based Biometric Person Authentication, 2003, ISBN : 978-3-540-40302-9
 - [18] A. K. Jain and H. Chen, "Matching of dental X-ray images for human identification," Pattern Recognition. vol. 37, pp. 1519–1532, 2004.
 - [19] H. Chen, A. K. Jain, and E. Lansing, "Tooth Contour Extraction for Matching Dental Radiographs," Proc. 17th Int. Conf. Pattern Recognition, 2004. ICPR 2004., vol. 3, no. 1, p. 522–525 Vol.3.
 - [20] H. Chen and A. K. Jain, "Dental Biometrics: Alignment and Matching of Dental Radiographs," IEEE Trans Pattern Anal Mach Intell. 2005 Aug;27(8):1319-26.
 - [21] V. Pushparaj and U. Gurunathan, "An Effective Dental Shape Extraction Algorithm Using Contour Information and Matching by Mahalanobis Distance," Journal of digital imaging, vol. 26, no. 2, pp. 259-268, 2013.
 - [22] V. Pushparaj, "Victim identification with dental images using texture and morphological operations." J. Electron. Imag. 23(1) 013004 (13 January 2014) <https://doi.org/10.1117/1.JEI.23.1.013004>
 - [23] P. L. Lin, P. W. Huang, Y. S. Cho, and C. H. Kuo, "An automatic and effective tooth isolation method for dental radiographs," Opto-Electronics Review 21 (2013): 126-136.
 - [24] V. F. Ferrario, C. Sforza, A. Miani, and G. Tartaglia, "Mathematical definition of the shape of dental arches in human permanent healthy dentitions," The European Journal of Orthodontics, vol. 16, pp. 287-294, August 1, 1994 1994.
 - [25] S. AlHarbi, E. A. Alkofide, and A. AlMadi, "Mathematical Analyses of Dental Arch Curvature in Normal Occlusion," The Angle Orthodontist, vol. 78, pp. 281-287, 2008.
 - [26] M. Camporesi, "Thin-plate spline analysis of arch form in a Southern European population with an ideal natural occlusion," The European Journal of Orthodontics, vol. 28, pp. 135-140, 2005.
 - [27] T. Kondo, S. H. Ong, and K. W. C. Foong, "Tooth segmentation of dental study models using range images," Medical Imaging, IEEE Transactions on, vol. 23, pp. 350-362, 2004.
 - [28] J. A. Kieser, V. Bernal, J. Neil Waddell, and S. Raju, "The uniqueness of the human anterior dentition: A geometric morphometric analysis," Journal of Forensic Sciences, vol. 52, pp. 671-677, 2007.